

The Causes of Geomagnetic Storms

Bruce T. Tsurutani

Space Physics and Astrophysics Section, Jet Propulsion Laboratory, California Institute of Technology, Pasadena, California, 91109

Walter D. Gonzalez

Instituto Nacional Pesquisas Espaciais, Sao Jose dos Campos, San Paulo, Brazil

I. SOLAR PHENOMENA

One of the oldest mysteries in geomagnetism is the linkage between solar and geomagnetic activity. Sabine (1852), first noted that both the numbers of sunspots and geomagnetic storms at Earth have an eleven year cycle. A few years later, Carrington (1860) reported that a large magnetic storm followed the great September 1859 solar flare and a causal relationship between flares and storms was speculated. It was not until this century that a well-accepted statistical survey on large solar flares and geomagnetic storms was performed (Newton, 1943). The results indicated that a significant correlation between flares and geomagnetic storms exist.

Although the two phenomena, one at the Sun and the other at the Earth, were statistically correlated, the exact physical linkage was still an unknown at this time. Various hypotheses were proposed. It was not until the Skylab white light coronagraph images were available, that large masses of coronal material were observed to be ejected from the Sun in association with solar flares (and prominence eruptions). The plasma link between the Sun and the Earth thus became well established.

Figure 1, is an example of one such solar ejection, called a Coronal Mass Ejection, or CME (Gosling et al., 1975). Although it was originally thought that the magnetic annihilation (which is the cause of solar flares) provided the energy for the expulsion of the coronal material, careful timing analyses demonstrated that the CMEs are released first, and thus flares are after-effects of the mass ejections (Harrison, 1986). This has led to some severe rethinking of how mass is ejected from the solar corona.

II. TYPES OF SOLAR WIND

There have been plasma and magnetic field instruments onboard interplanetary spacecraft since the early 1960s. These experiments discovered that there is a continuous flow of plasma coming outward from the Sun. At 1 Astronomical Unit (the Earth's distance from the Sun), this "solar wind" has a nominal velocity of $\sim 400 \text{ km s}^{-1}$ and a density of $\sim 8 \text{ to } 10 \text{ particles cm}^{-3}$. The plasma consists of primarily hot electrons ($T_e \sim 1.5 \times 10^5 \text{ K}$) and protons ($T_p \sim 0.8 \times 10^4 \text{ K}$).

with a minor fraction ($\sim 3\text{-}5\%$) of 1 le^{+4} ions. The plasma has an embedded magnetic field of intensity $\sim 5\text{ nT}$. At Earth, 1 AU from the Sun, the typical plasma to magnetic field energy density ratio, β ($8\pi nkT/B^2$), is roughly 1.0.

Besides the quiescent solar wind discussed above, at times near solar maximum (by definition when there is a maximum number of sunspots), high speed streams occur with velocities occasionally greater than 600 km s^{-1} and sometimes even greater than $1,000\text{ km s}^{-1}$. Approximately 90% of these events are associated with CMEs. Because the ambient magnetosonic wave speed is only $\sim 100\text{ km s}^{-1}$, the difference in flow velocity between the faster stream and the slower stream is greater than the magnetosonic (fast mode) speed. Thus, a fast forward shock is formed at the leading edge of the high-speed stream.

A schematic of the shock and driver gas is shown in Figure 2. The shock is the outermost (antisunward) extension of the solar disturbance's propagation into interplanetary space. The region immediately behind (sunward of) the shock is composed of swept-up, compressed and accelerated plasma and fields from the "slow" stream and is called the "sheath" region. Behind this is the driver gas (CME) proper. The driver gas has previously been identified by a variety of signatures: enhanced Helium/hydrogen density ratios, low ion temperatures, high intensity magnetic fields with low variances and bi-directional streaming, of thermal ions and electrons. It should be mentioned that no one measurement or combination of measurements have proved to be a perfect means of identification, however (Zwick et al., 1983; Choe et al., 1992). Intense research in this area is still ongoing.

Because of the typically high intensity magnetic fields ($10\text{-}50\text{ nT}$) and low plasma temperatures, the driver gas is a low beta plasma, $\beta = 0.03 - 0.8$, in about 10% of the cases, the magnetic field in these regions has an unusual configuration, with large out-of-the ecliptic components. This has been named a magnetic cloud (Klein and Burlaga, 1982). A recent schematic of the magnetic field configuration is shown in Figure 3 (Marubashi, 1986). When crossing the cloud, the field rotates from north-to-south or south-to north with a time scale of a day or longer. This configuration is force-free, supported only by field-aligned currents flowing inside of it.

One fundamental question concerning this magnetic field region is whether it is "closed" like a magnetic bubble, or whether it is a loop with both ends remaining attached to the Sun. The presence of bi-directional streaming electrons and protons in this region have been used to argue for a closed magnetic structure. However, the observations of energetic solar flare particles both outside and inside of this structure and the small amount of modulation of cosmic rays by these structures, have been used to argue for an open structure still connected back to the Sun (Kahler and Reames, 1991). The argument about open or closed structures persists because one-

spacecraft "cuts" through the three-dimensional structure cannot resolve such a question. Multi-spacecraft measurements are needed.

111. MAGNETIC RECONNECTION AND MAGNETIC STORMS

The high speed plasma events which are led by shocks, followed by plasma sheaths and then the driver gases, do not have direct access to the Earth's dayside atmosphere and ionosphere. The protective magnetosphere which is created by the internal magnetic field of the Earth, deflects the interplanetary plasma and fields, so the latter flow around the magnetosphere. The solar wind plasma primarily enters the magnetosphere through magnetic connection between the interplanetary magnetic fields and the Earth's outer fields, as schematically shown in Figure 4. When the interplanetary magnetic field (IMF) has a component with a direction opposite (southward) to the magnetospheric fields (northward), inter-connection can take place, and the solar wind convects these fields back into the tail region where they reconnect once more (Dungey, 1961; Vasyliunas, 1975). The magnetic tension on the freshly reconnected tail fields "snaps" the reconnected fields and plasma forward toward the nightside of the Earth. The convection process, through conservation of the first two adiabatic invariants (μ and $\oint \mathbf{p} \cdot d\mathbf{s}$), energizes the plasma. When the magnetic dayside connection is particularly intense, the nightside reconnection is also correspondingly high, and the plasma is driven deep into the nightside magnetosphere. Because the plasma is anisotropically heated by this process, plasma instabilities (loss-cone instabilities) occur, creating electromagnetic and electrostatic plasma waves, which cyclotron resonate with the energetic particles (Kennel and Petschek, 1966). The wave-particle interactions break the particles' first adiabatic invariant, scattering them in pitch angle. Particles that have their mirror points lowered to altitudes at atmosphere/ionosphere heights are lost by collisions. In the loss process, atmospheric and ionospheric atoms and molecules are excited, resulting in characteristic auroral emissions. The above scenario is the cause of the diffuse aurora, a phenomenon which occurs primarily in the Earth's midnight-to-dawn sector. The spreading of the aurora toward local dawn is caused by the electron azimuthal drifts, a topic that will be discussed shortly.

The nightside convection electric field which drives the plasma from the tail into the nightside magnetosphere has a dawn-to-dusk orientation. When this field develops discontinuities with $\nabla \cdot \mathbf{E} < 0$, magnetic field-aligned currents with associated field-aligned electric potential differences and electron precipitation develop. This powers the ~ 100 km scale auroral precipitation (Lyons, 1980; 1992). Auroras of this type are shown in Figure 5.

As the energetic particles are convected deep into the Earth's nightside magnetosphere, they are also subjected to magnetic field curvature and gradient forces. These two forces act in unison

for the same charge sign, and the net effect is that protons drift from midnight toward dusk and electrons from midnight toward dawn (Figure 6). This oppositely directed drift comprises a ring of current (the ring current) around the Earth. The current is a diamagnetic one, decreasing the intensity of the Earth's field, as measured at the equator. An enhanced ring current is the prime indicator of a magnetic storm. The total energy of the particles in the ring current (measured by the intensity of the diamagnetic field perturbation), is a measure of the storm intensity (Dessler and Parker, 1959).

WC now compare the interplanetary features discussed previously and their relationships to the phases of a magnetic storm, shown in Figure 7. In the Figure, the ordinate gives the change in the horizontal component of the Earth's magnetic field, measured by a chain of ground based stations located near the equator (the ordinate is the field averaged over these stations). The abscissa gives time. There are three phases to a geomagnetic storm, as indicated in the Figure. They are called the initial phase, where the horizontal component increases to positive values of up to 10's of nT, a main phase which can have magnitudes of negative hundreds of nT, and a recovery phase where the field gradually returns back to the ambient level. An average of these deviations from the field ambient value is called the DST index, measured in nT. The time scales of the three phases are indeterminate. The initial phase can last minutes to many hours, the main phase a half-hour to several hours, and the recovery from tens of hours to a week.

The initial phase is caused by the solar wind ram pressure ($\frac{1}{2} \rho V_{sw}^2$) increase as the interplanetary shock wave hits the frontside magnetosphere. There are both abrupt velocity and plasma density increases across the shock that lead to the dramatic ram pressure increase. This pressure pulse rapidly compresses the magnetosphere and causes the increase in the average field at the equator.

The storm main phase onset is initiated by a southward IMF and consequential enhanced magnetic reconnection. Due to enhanced nightside convection, the Van Allen radiation belt particles increase in number and average energy. As the ring current increases, the diamagnetic current causes the decrease in the Earth's field.

The third, or recovery, phase of the storm is due to the decay of this belt of energetic particles. There are four fundamental mechanisms for this loss: 1) wave-particle interactions, where waves pitch-angle scatter the particles into the "loss cone", 2) for charged particles with low mirror points or those trapped on field lines within the plasmasphere (a region of high density plasma), Coulomb interactions take place, 3) charge exchange with neutrals is a dominant loss mechanism, particularly at large L, and 4) convection across the dayside magnetopause will lead to loss within the magnetosheath. The first three processes occur within the storm main and recovery phase. The fourth mechanism only occurs during the main phase. During particularly intense storm main phases when the loss time scales can be as rapid as an

hour or less, the only possible mechanism is wave-particle interactions. This has not been observationally confirmed, however.

One type of aurora, which is specifically associated with magnetic storms, is the brilliant "blood" red aurora shown in Figure 8. The red aurora is created by the emission of a 6300 Å oxygen line and occurs at very high altitudes (200-600 km) where the collisional de-excitation time scales are larger than the metastable decay time of ~ 200 s. One thought (Cornwall et al., 1971) is that electromagnetic ion cyclotron waves generated by the loss cone instability of the ring current protons get damped and accelerate the magnetospheric thermal electrons up to energies of 2-3 eV. These low energy electrons are stopped high in the atmosphere resulting in the aurora. Another possibility (Fok et al., 1991) is that ring current ions and electrons are scattered and slowed down by Coulomb interactions with thermal plasma and are eventually removed from trapped orbits. There is now more evidence pointing toward the latter mechanism.

IV. AN INTERPLANETARY EXAMPLE

Previously, in Figure 2, we showed the profile of the two primary regions where intense southward interplanetary magnetic fields can occur within the high-speed streams: in the sheath region behind the shock, and in the driver gas. We showed that a flux-rope configuration could lead to large southward (and northward) field orientations, magnetic connection at the Earth's magnetosphere (when the IMF is southward), and aurora. Figure 9 illustrates five observed and hypothesized mechanisms for sheath southward fields. Preexisting southward fields can simply be (a) compressed by the shock, (b) the heliospheric current sheet which separates the northern and southern heliospheric fields can be distorted and compressed by shock compression, and (c) large amplitude waves and turbulence or the presence of discontinuities can be associated with out-of-the-ecliptic field components, (d) the sheath plasma flows around the driver gas, the magnetic fields will drape over it, much like the field draping around a comet. The magnetic tension will expel plasma down the lines of force creating a low beta region near the stagnation region (Zwan and Wolf, 1976). Finally, (e) a mechanism has been demonstrated for creating large scale north-south fields from flows around an object like a driver gas. The illustration gives an example of this.

It should be noted that in the two regions, the sheath and the driver gas, the field orientation has been empirically found to be northward-directed with equal probability as for southward orientations. There are also cases where the field lies primarily in the ecliptic as well as cases with large north-south components which vary rapidly in time. The latter cases do not cause storms because of their short reconnection/convection time scales. The result is that only one in

about 6 cases of CMEs that impinge upon the Earth lead to an intense ($D_{ST} < -100$ nT) magnetic storm (Tsurutani and Gonzalez, 1990).

Many of the solar wind-magnetic storm relationships discussed above can be illustrated by showing some space plasma data. An example is given in Figure 10. From top to bottom, the panels give the solar wind velocity, plasma density, magnetic field magnitude, two components of the magnetic field in GSE coordinates, the Auroral Electrojet index (AE) and D_{ST} . In the GSE coordinate system, x -points toward the Sun, y is in the ecliptic plane pointing in the direction of rotation of the planets, and z completes the right-hand system. The AE index is an ionosphere current which flows at ~ 100 km altitude and is typically located at auroral latitudes (~ 63 - 68° magnetic latitude). This current becomes particularly intense during active auroral displays and can reach amplitudes of up to 10^6 Amperes. The AE index is a ground-based measurement of the magnetic field associated with this current.

An interplanetary shock is noted in the Figure at the beginning of August 27 by an abrupt jump in the solar wind velocity, density and magnetic field magnitude. The increase in ram pressure leads to an increase in D_{ST} to positive values. This is the onset of the storm initial phase. Towards the end of the day, B_z turns negative (southward) and remains in this direction for over 12 hours. D_{ST} increases in response, signifying the storm main phase, i.e., the ring current build-up. As the B_z turns positive (northward), D_{ST} begins to increase and the onset of the recovery phase begins.

In this event, the storm recovery phase is exceptionally long. Continuous auroral activity (AE) is associated with this interval and is illustrated by the bar in the AE panel. During this time, the interplanetary medium is characterized by rapid fluctuations in the transverse (y and z) components of the magnetic field. The field magnitude is relatively constant. Analyses of the field and plasma data indicate that these fluctuations are Alfvén waves (Belcher and Davis, 1971) propagating outward from the sun. Use of magnetic field measurements on spacecraft closer to the Earth have demonstrated that the AE increases are correlated with southward deviations of the field, the latter associated with the Alfvén waves. Thus, the auroral (AE) activity is due to magnetic reconnection (Tsurutani et al., 1990). However, it is noted that there is very little ring current activity (D_{ST}) during this extended interval.

The effect of the Alfvén waves upon the magnetosphere can be understood by the nature of the southward field components. The fields are less intense than those during the storm main phase (see Figure) and their durations are considerably shorter. Thus the consequential nightside convection will be of lower velocity and will occur sporadically. Plasma will only be brought into the outer regions of the magnetosphere where they feed the high latitude aurora and not deep into the magnetosphere where the ring current predominantly resides.

Other types of solar wind-magnetospheric interactions had been hypothesized, such as a "viscous interaction" between the solar wind and the magnetosphere (Axford and Hines, 1961; Sonnerup, 1980). There is evidence that the Kelvin-Helmholtz instability occurs when the IMF is orthogonal (northward to the tail field direction). However, it was recently shown that only ~ 0.1 % of the solar wind ram energy enters the magnetosphere during these events, as compared to 10% during magnetic reconnection (storm events).

Another "viscous type" of interaction is resonant wave-particle interactions near the dayside magnetopause. It has been shown that electromagnetic and electrostatic waves can scatter magnetosheath plasma across this boundary at a rate which approaches 10% of the Bohm diffusion rate (Tsurutani and Thorne, 1982). The diffusion and pitch angle scattering have been speculated to be the cause of the dayside aurora, a low-level feature which is almost always present.

V. FUTURE SPACE PHYSICS AND AERONOMY MISSIONS

Where do we go from here? How are we going to fully understand the flow of energy from the sun to the magnetosphere and the eventual sinks in the ionosphere and magnetotail? One future space mission is the International Solar Terrestrial Physics (ISTP) mission which is devoted to quantitatively solve the energy flow problem discussed in this paper. The National Aeronautics and Space Administration (NASA), European Space Agency (ESA), Russian Space Research Institute (IKI) and Japanese Institute of Space and Astronautical Science (ISAS) scientists will place spacecraft in interplanetary space (WIND, SOHO and Cluster), in the magnetosphere (Polar, and Cluster) and in the tail (GEOTAIL) to do this energy mapping.

Lastly, a mission of the future is the Small Solar Probe spacecraft. This mission is being considered as another joint NASA/ESA/IKI/ISAS mission. The Small Solar Probe is designed to go to a distance as close as 3 solar radii from the sun where the external temperature reaches ~2100 K, a temperature that will melt most metals or at least make them limp or brittle. The carbon-carbon heat shield will protect the scientific instruments which are located in the shield's umbra, and will allow them to operate at temperatures of ~ 20° C. The international complement of instruments will measure fields and particles in situ to establish the cause(s) of coronal heating and the acceleration of the solar wind, determine the characteristics of microflares and possibly even detect the release of a CME. This mission will probe one of the two remaining frontiers of our heliosphere.

ACKNOWLEDGMENTS

We wish to thank S. Kahler, R. Thorne and G. Bering for scientific discussions concerning several parts of this paper. The work represented in this paper was performed in part at the Jet Propulsion Laboratory, California Institute of Technology, Pasadena, (California under contract with the National Aeronautics and Space Administration.

REFERENCES

- Axford, W. I. and C. O. Hines, A unified theory of high-latitude geophysical phenomena and geomagnetic storms, Can. J. Phys., 39, 1433, 1961.
- Bame, S. J., J. R. Asbridge, W. C. Feldman, E. E. Fenimore, and J. T. Gosling, Solar wind heavy ions from flare-heated coronal plasma, Solar Phys., 62, 179, 1979.
- Belcher, J. W. and L. Davis, Jr., Large amplitude Alfvén waves in the interplanetary medium, 2., J. Geophys. Res., 76, 3534, 1971.
- Carrington, R. C., Mon. Not. Roy. Astron. Soc., 20, 13, 1860.
- Choe, G. S., N. LaBelle-Hamer, H. Tsurutani and L. C. Lee, Identification of a driver gas boundary layer, EOS, 73, 485, 1992.
- Cornwall, J. M., F. V. Coroniti and R. M. Thorne, Turbulent loss of ring current protons, J. Geophys. Res., 75, 4699, 1970.
- Cornwall, J. M., F. V. Coroniti and R. M. Thorne, Unified Theory of SAR formation at the plasmapause, J. Geophys. Res., 76, 4428, 1971.
- Dessler, A. J. and E. N. Parker, Hydromagnetic theory of geomagnetic storms, J. Geophys. Res., 64, 2239, 1959.
- Dungey, J. W., Interplanetary magnetic field and the auroral zones, Phys. Rev. Letts., 6, 47, 1961.

- Fok, M. C., J. U. Kozyra, A. F. Nagy, and '1'. E. Cravens, Lifetimes of ring current particles due to Coulomb collisions in the plasmasphere, J. Geophys. Res., 96, 7861, 1991.
- Gonzalez, W. D. and B. T. Tsurutani, Criteria of interplanetary parameters causing intense magnetic storms ($D_{ST} < -100$ nT), Planet. Space Sci., 35, 1101, 1987.
- Gonzalez, W. D., A. L. C. Gonzalez, O. Mendes, Jr., and B. T. Tsurutani, Difficulties defining storm Sudden commencements, EOS, 73, 180, 1992.
- Gosling, J. T., E. Hildner, R. M. McQueen, R. H. Munro, A. I. Poland and C. I. Ross, Solar Phys., 40, 439, 1975.
- Harrison, R. A., Solar coronal mass ejection and flares, Astron. Astrophys., 162, 283, 1986.
- Kahler, S. W. and D. V. Reames, Probing the magnetic topologies of magnetic clouds by means of solar energetic particles, J. Geophys. Res., 96, 9419, 1991.
- Kennel, C. F., and H. E. Petscheck, Limit on stably trapped particle fluxes, J. Geophys. Res., 71, 1, 1966.
- Klein, L. W. and L. F. Burlaga, Interplanetary magnetic clouds at 1 A.U., J. Geophys. Res., 87, 613, 1982.
- Lyons, L. R., Generation of large-scale regions of auroral currents, electric potentials and precipitation by the divergence of the convection electric field, J. Geophys. Res., 85, 17, 1980.
- Lyons, L. R., Formation of auroral arcs via magnetosphere-ionosphere coupling, Res. Geophys., 30, 93, 1992.
- Marubashi, K., Structure of the interplanetary magnetic clouds and their solar origins, Adv. Space Res., 6, 335, 1986.
- Newton, H. W., Mon. Not. Roy. Astron. Soc., 103, 244, 1943.

Sabine, E., Philos. Trans. R. Soc. London, 142, 103, 1852.

Tsurutani, B. T. and R. M. Thorne, Diffusion processes in the magnetospheric boundary layer, Geophys. Res. Lett., 9, 1247, 1982.

Tsurutani, B. T. and W. D. Gonzalez, Reply, J. Geophys. Res., 95, 12305, 1990.

Tsurutani, B. T., T. Gould, B. E. Goldstein, W. D. Gonzalez, and M. Suguira, Interplanetary Alfvén waves and auroral (substorm) activity: IMP 8, J. Geophys. Res., 45, 2241, 1990.

Williams, D. J., Dynamics of the Earth's ring current: theory and observation, Space Sci. Rev., 42, 375, 1985.

Vasyliunas, V. M., Theoretical models of magnetic field line merging, 1, Rev. Geophys. Space Phys. 13, 303, 1975.

Zwan, B. J. and R. A. Wolf, Depletion of Solar wind plasma near a planetary boundary, J. Geophys. Res., 81, 1636, 1976.

Zwickl, R. D., J. R. Asbridge, S. J. Bame, W. C. Feldman, J. T. Gosling, and E. J. Smith, Plasma properties of driver gas following interplanetary shocks observed by ISEE-3, Solar Wind Five, 711, 1983.

Suggested Reading:

Hundhausen, A. J., Coronal Expansion and Solar Wind, Physics and Chem. in Space, Springer Verlag, N.Y. 5, 1972.

Neugebauer, M., Quasi-stationary and transient states of solar wind, Science, 252, 404, 1991.

Figure Captions

Fig. 1. The March 18, 1989 coronal mass ejection. Courtesy of A. Hundhausen.

Fig. 2. A schematic of a plasma driver gas, sheath and shock. Propagation is to the right. At the core of the driver gas is a low β region characterized by low field variances, low plasma temperatures and Helium enhancements. "There is sometimes a Helium shell around this low beta region. The shape of the driver has been determined by magnetic field normal analyses. From Choe et al. (1992).

Fig. 3. A possible configuration of the magnetic fields within the low beta portion of the driver gas. Taken from Marubashi (1986).

Fig. 4. Magnetic reconnection between interplanetary and magnetospheric magnetic fields.

Fig. 5. An example of the aurora borealis. Taken in Fairbanks, Alaska by S.-I. Akasofu.

Fig. 6. Energetic particle motions: gyration, bounce and drift. Taken from Williams (1985).

Fig. 7. The three phases of a magnetic storm. See discussion in Gonzalez et al. (1992).

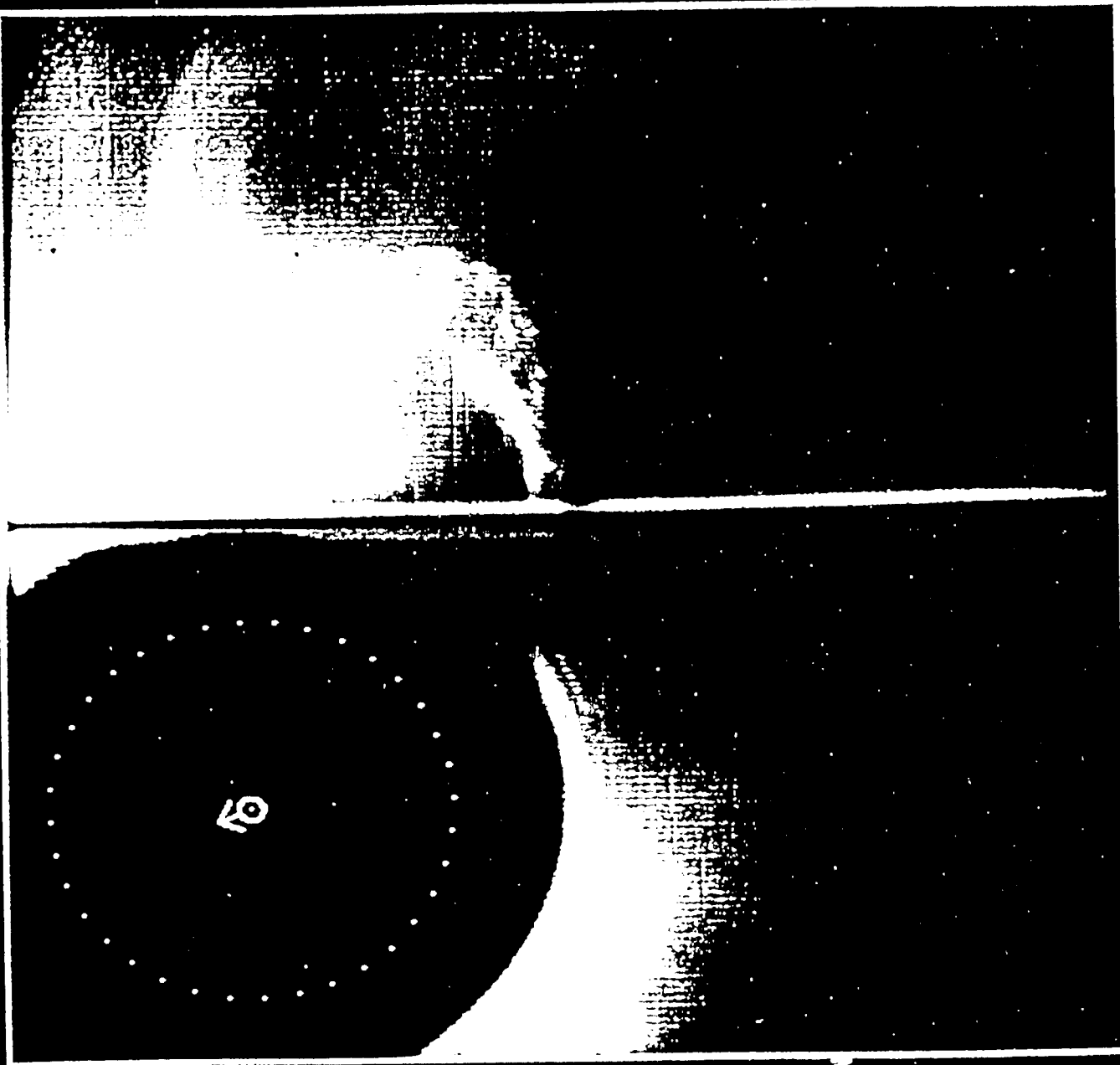
Fig. 8. A red aurora. These aurora can occur at low latitudes and are associated with magnetic storms. Courtesy of Vic Hessler of the Geophysical Institute, University of Alaska, Fairbanks, AK.

Fig. 9. The various proposed causes of southward magnetic fields in the sheaths of high-speed interplanetary streams.

Fig. 10. An example of a solar flare-related high speed interplanetary stream and its geomagnetic effects. Taken from Tsurutani et al. (1988).

Fig. 11. The Solar Probe/Piccoll mission.

DATE 89: 077
TIME 03:34:50
18 MAR 1989
FILTER GREEN
POLAROID CLR
SECTOR 5
EXPOSURE 6
RESOLUTION LOW
ROLL -20
FRAME 2049



+
HRO/SMM CORONAGRAPH / POLARIMETER

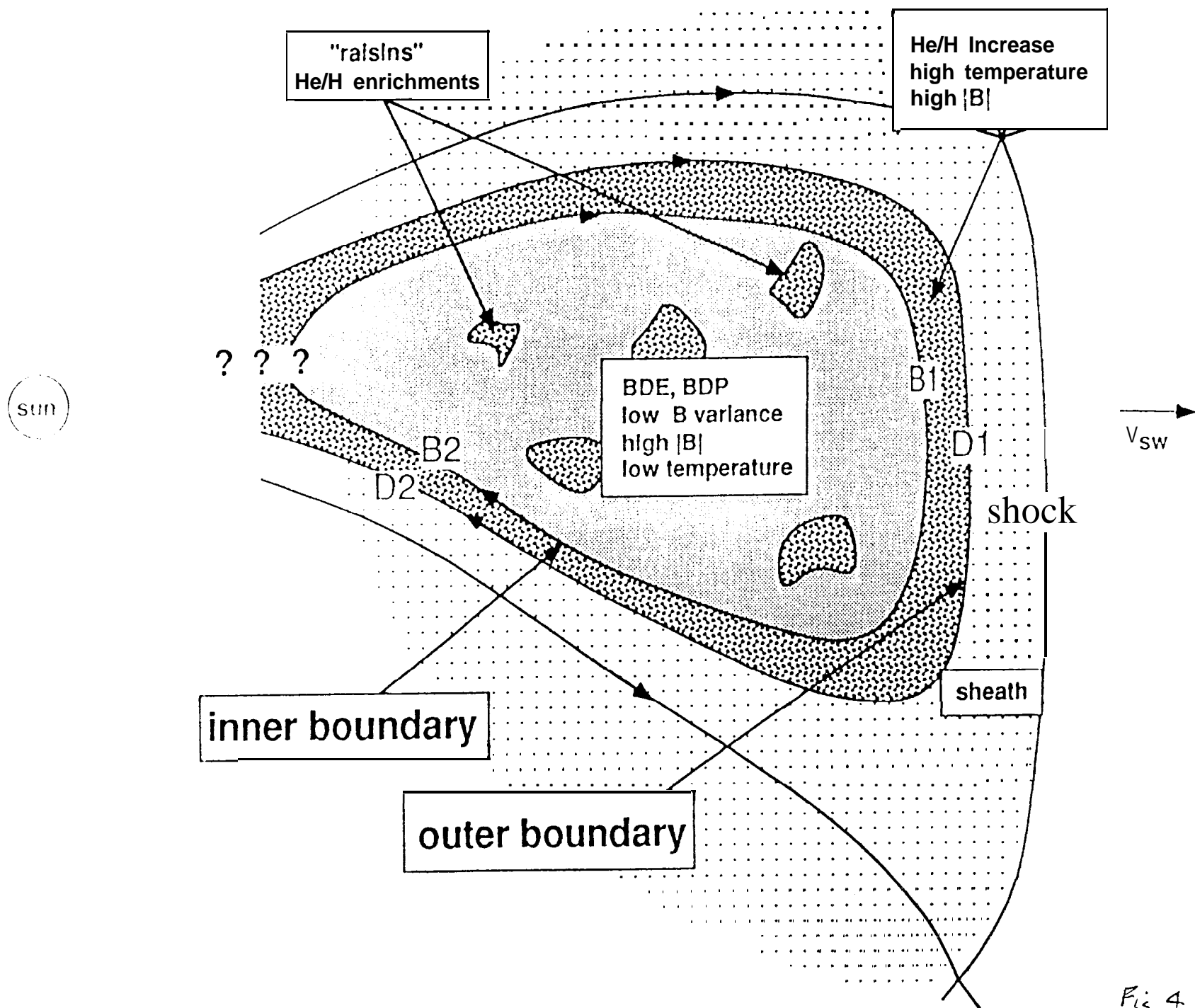


Fig 4

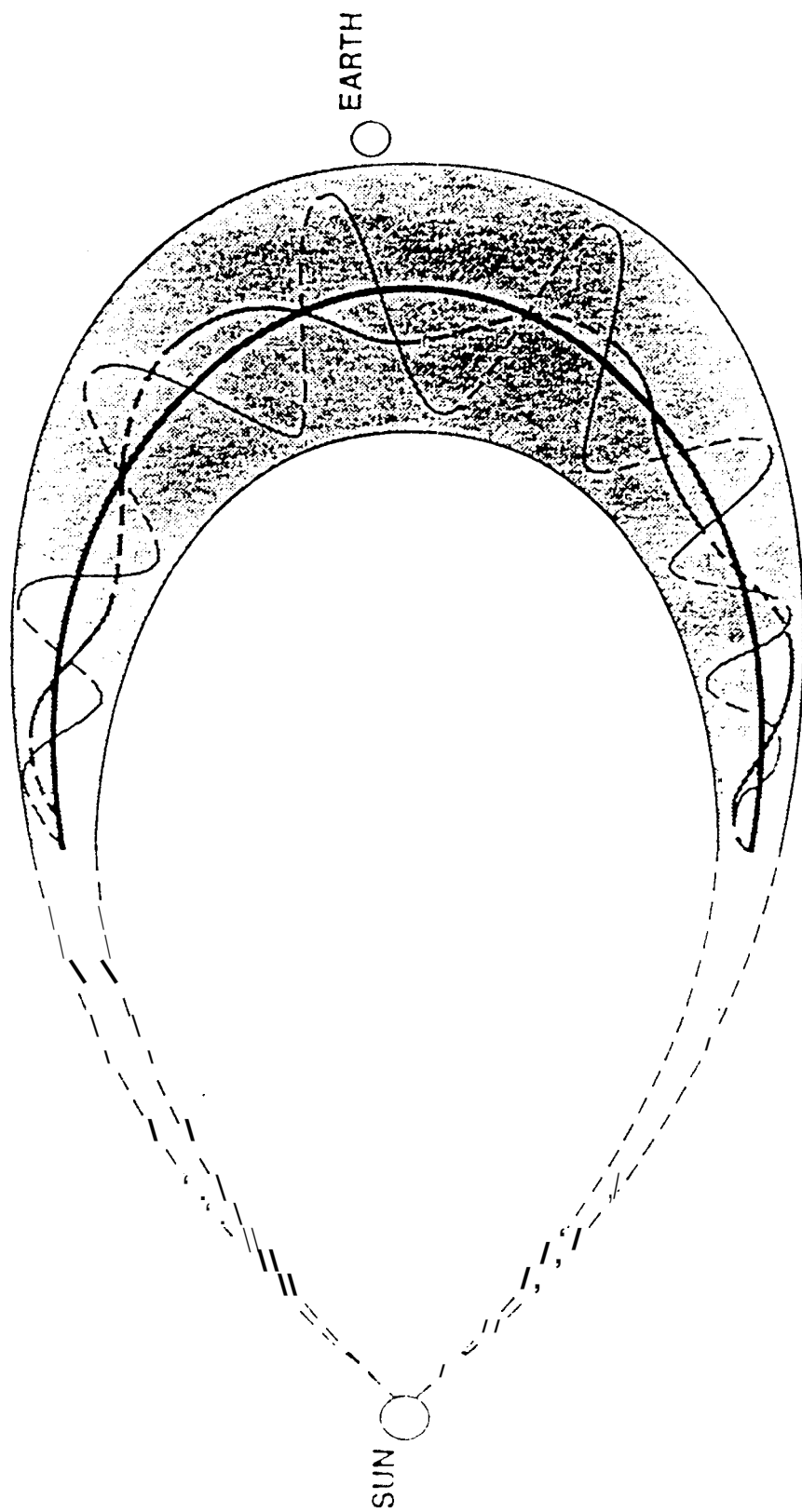


Fig 3

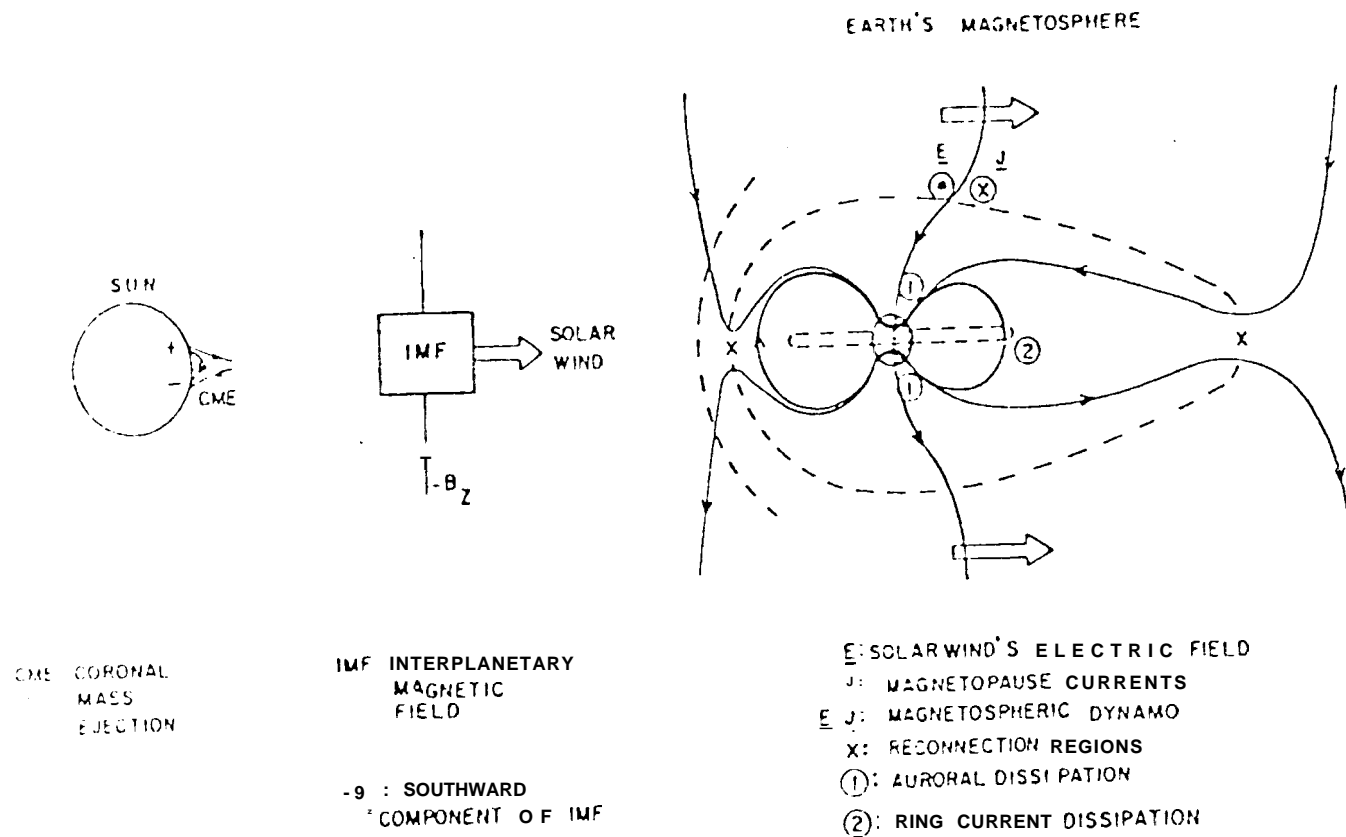


Fig 6



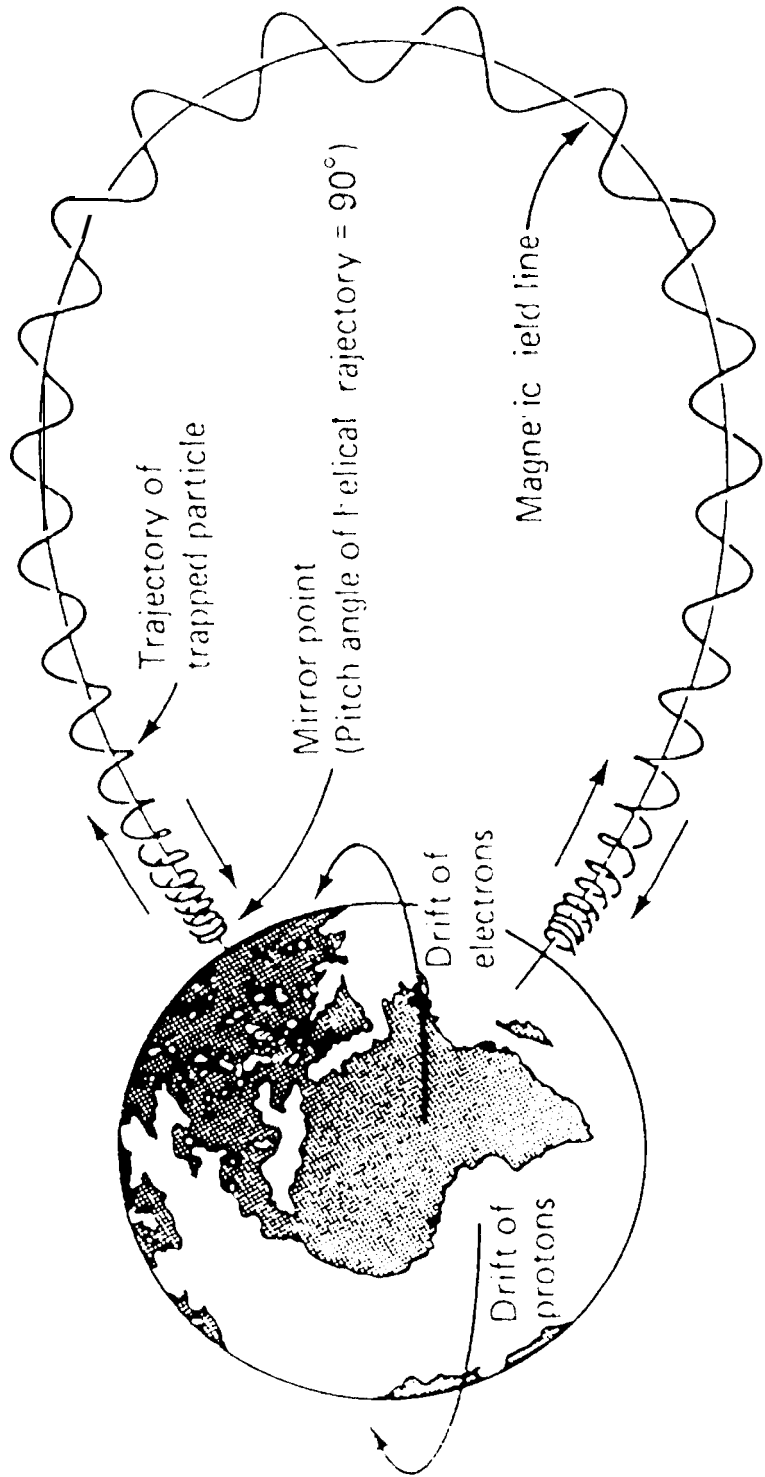


Fig 8

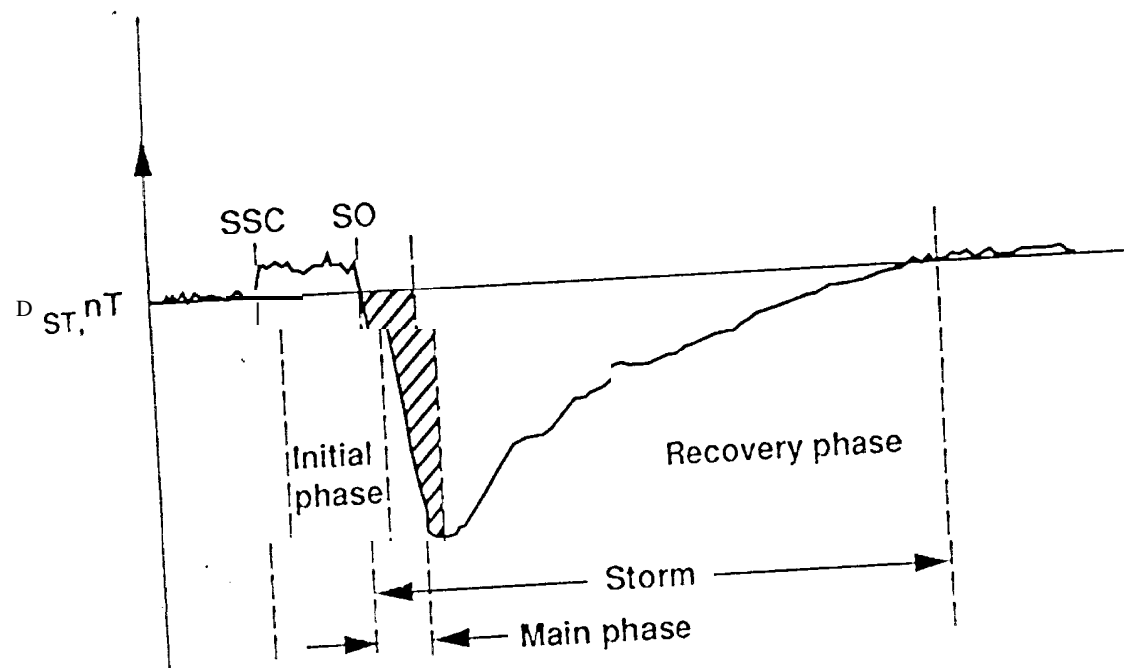
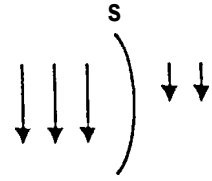


Fig 9

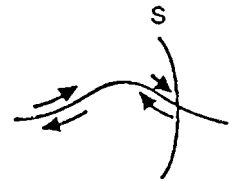


SHEATH FIELDS

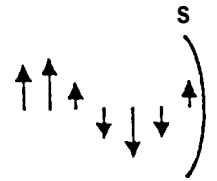
- a) Shocked southward fields
Tsurutani et al., 1988



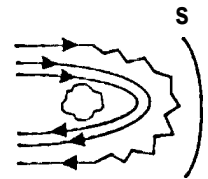
- b) Shocked heliospheric current sheets
Tsurutani et al., 1984



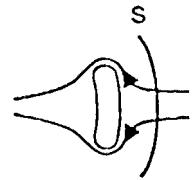
- c) Turbulence, waves or discontinuities



- d) Draped magnetic fields
Zwan and Wolf, 1976

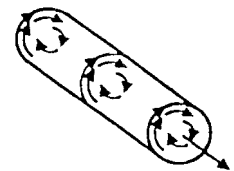


McComas et al., 1989

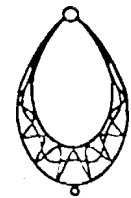


DRIVER GAS FIELDS

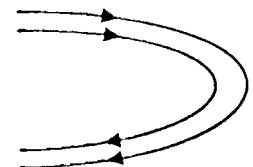
- e) Magnetic clouds
Klein and Burlaga, 1982



Fluxropes
Marubashi, 1986



Magnetic tongues
Gold, 1962



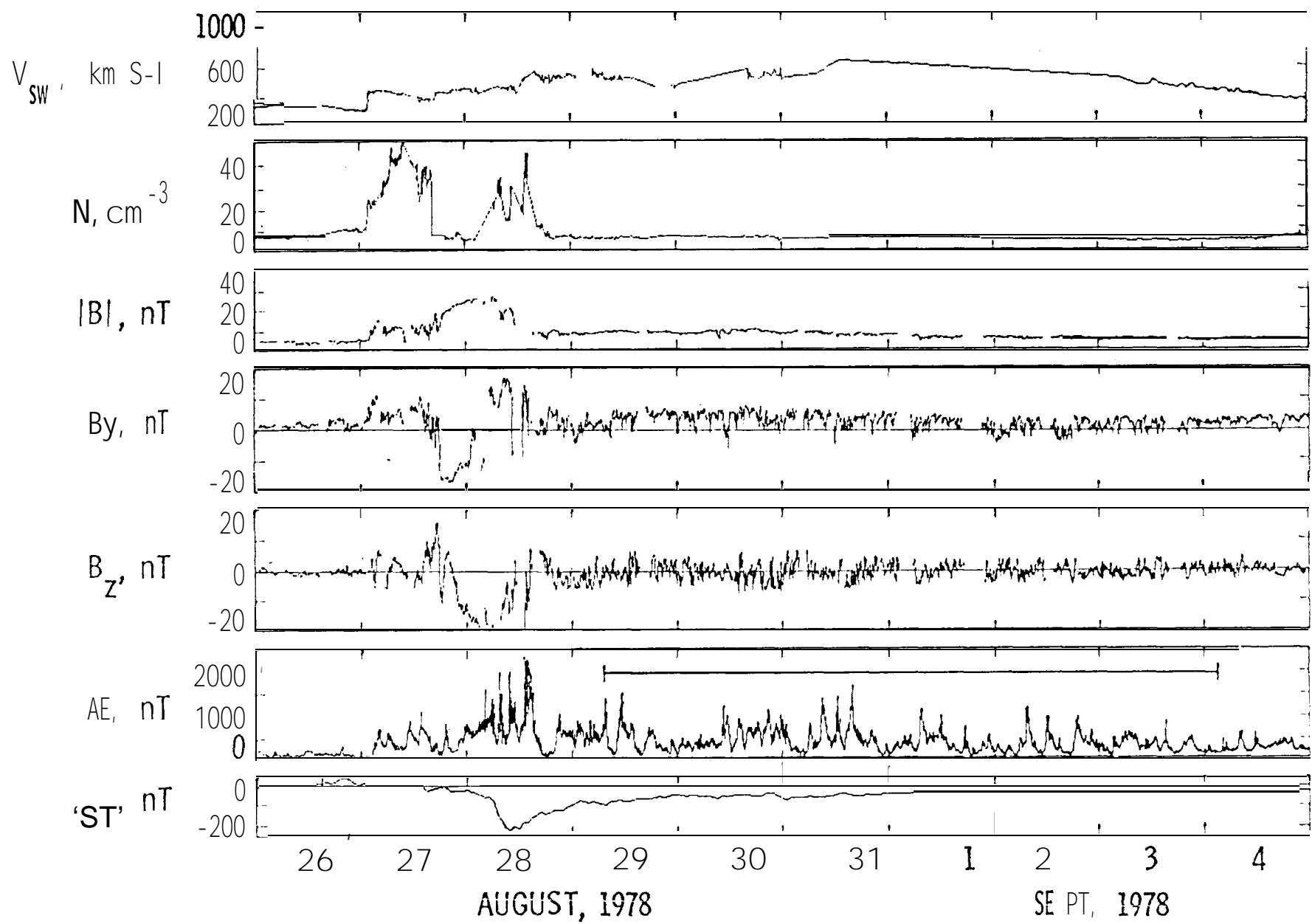


Fig 12